

Measurement of muon momentum resolution of the ATLAS detector

Antonio Salvucci^{1,a} on behalf of the ATLAS Collaboration

Radboud University Nijmegen and Nikhef

Abstract. The ATLAS detector has been designed to have good muon momentum resolution up to momenta in the TeV range. The muon momentum resolution of the ATLAS spectrometer has been measured with p - p collision data recorded in 2011. The measurement combines the di-muon mass resolution in $J/\psi \rightarrow \mu\mu$ and $Z \rightarrow \mu\mu$ decays with measurements of the alignment accuracy of the detector based on straight muon tracks, which are acquired with special runs without magnetic field in the ATLAS detector.

1 Introduction

The physics programme of the ATLAS Experiment [1] at the LHC includes investigations of many processes with final state muons. The ATLAS detector is equipped with a Muon Spectrometer (MS) optimized to provide a momentum measurement with a relative resolution better than 3% over a wide p_T range and 10% at $p_T = 1$ TeV, where p_T is the muon momentum component in the plane transverse to the beam axis. The momentum in the MS is measured from the deflection of the muon trajectory in the magnetic field generated by a system of air-core toroid coils. The MS track is reconstructed using three layers of precision drift tube (MDT) chambers in the pseudorapidity¹ range $|\eta| < 2$, and two layers of MDT chambers behind one layer of cathode strip chambers (CSC) for $2 \leq |\eta| < 2.7$.

An additional determination of the muon momentum is provided by the Inner Detector (ID) for $|\eta| < 2.5$. The ID is composed of three detectors providing coordinate measurements for track reconstruction inside a solenoidal magnetic field of 2 T. Close to the interaction point it features a silicon pixel detector, surrounded by a silicon strip detector (SCT). In the outermost part there is a transition radiation straw tube tracker (TRT) with a coverage of $|\eta| < 1.9$.

Muons entering in this analysis are reconstructed as *combined muons*. The underlying muon identification is described in [2] and relies on the principle that first separate tracks are measured in ID and MS before they are reconstructed as a single trajectory. This yields a higher momentum resolution than could be achieved using the individual tracks.

This paper documents the muon momentum resolution in the first pass of reconstruction of p - p collision data collected in 2011 corresponding to an integrated luminosity of 2.54 fb^{-1} . The first pass of reconstruction uses preliminary calibration and alignment.

^a e-mail: a.salvucci@science.ru.nl

¹ The pseudorapidity is $\eta = -\ln(\tan(\theta/2))$, where θ is the polar angle with respect to the beam line.

2 Parametrization of the momentum resolution as a function of p_T and η

The relative momentum resolution, $\sigma(p)/p$, originates from different effects [3,4]. The ATLAS MS is designed to provide a momentum resolution as a function of the η and ϕ . For a given value of η , the resolution can be parametrized as a function of p_T :

$$\frac{\sigma(p)}{p} = \frac{p_0^{MS}}{p_T} \oplus p_1^{MS} \oplus p_2^{MS} \cdot p_T \quad (1)$$

where p_0^{MS} , p_1^{MS} , p_2^{MS} are coefficients related to the energy loss in the calorimeter material, multiple scattering and intrinsic resolution terms, respectively.

For the ID, the curvature measurement depends on the track length of the muon in the active material, which is reduced close to the edge of the TRT fiducial volume. This results in a uniform response in the central part and a rapid worsening beyond this region. The approximate parametrization of the resolution is

$$\frac{\sigma(p)}{p} = p_1^{ID} \oplus p_2^{ID} \cdot p_T \quad \text{for } |\eta| < 1.9 \quad (2)$$

$$\frac{\sigma(p)}{p} = p_1^{ID} \oplus p_2^{ID} \cdot p_T \frac{1}{\tan^2(\theta)} \quad \text{for } |\eta| > 1.9 \quad (3)$$

where p_1^{ID} , p_2^{ID} are the multiple scattering and the intrinsic resolution terms, respectively.

In this study, four regions in pseudorapidity are distinguished:

- *Barrel*: covering $0 < |\eta| < 1.05$;
- *Transition*: covering $1.05 < |\eta| < 1.7$;
- *End-caps*: covering $1.7 < |\eta| < 2.0$;
- *CSC/No-TRT*: covering $2.0 < |\eta| < 2.5$.

These four regions are studied using $Z \rightarrow \mu\mu$ decays.

3 Combined fit to the muon resolution components

The process $Z \rightarrow \mu\mu$ is used to study the momentum resolution and to determine the corrections needed for simulation in each η region of the detector. We use two quantities:

- i) the width of the reconstructed di-muon invariant mass peak at the Z pole, which is a convolution of the natural width of the Z boson and the muon momentum resolution;
- ii) the difference between the independent momentum measurements of the ID and MS for combined muons, which is sensitive to the quadratic sum of the ID and MS momentum resolutions. This difference is weighted by the muon electric charge ($q/p_T^{ID} - q/p_T^{MS}$): this disentangles systematic effects of the curvature due to local misalignments from the overall intrinsic resolution, reducing the bias on the estimation of the resolution and correction parameters.

3.1 Global fit procedure

Using the previous inputs, the measurements of the MS and ID momentum resolution are obtained using a Monte Carlo template technique, based on a “global” fit procedure with:

- i) *a template fit to reconstructed Z lineshape*: we allow for momentum resolution smearing in the fit to the Z lineshape obtained from MS and ID tracks and a combined fit with events with muons in different detector regions. In this case we are sensitive to $\sigma_{mult.scatt.} \oplus \sigma_{intrinsic}$
- ii) the above, plus *template fit to $(q/p_T^{ID} - q/p_T^{MS})$ distribution*: we allow for momentum resolution smearing in the fit, that compute several bins of p_T , keeping regions separated. This case is sensitive to $\sigma_{ID} \oplus \sigma_{MS}$
- iii) *external constraints on MS alignment and multiple scattering in ID and MS* (see 3.2)

Concerning the smearing, for both the MS and the ID, the transformation of p_T is

$$p'_T = p_T \left(1 + g\Delta p_1^{ID,MS} + g\Delta p_2^{ID,MS} p_T \right) \quad (4)$$

where p'_T indicates the simulated muon p_T after applying the correction $\Delta p_i^{ID,MS}$, while g is a normally distributed random number with mean 0 and width 1.

3.2 External constraints to the combined fit

In the fitting procedure, additional knowledge is introduced from independent studies, both for the ID and the MS. This reduces the correlation among the multiple scattering and the detector resolution terms in the fit, resulting in smaller uncertainties on the fitted parameters.

For the ID, the correction to the multiple scattering term in the ID, Δp_1^{ID} , is fixed to a value of zero, due to a knowledge of the ID material of 0.05%.

For the MS, the multiple scattering term, Δp_1^{MS} , is a free parameter of the fit. The energy loss of muons is mainly concentrated in the calorimeter and has been measured in [6]. Its contribution to the overall MS resolution in the p_T range from 20 GeV to 100 GeV is negligible and so no additional contribution for the energy loss, Δp_0^{MS} , is included. For the intrinsic resolution term, Δp_2^{MS} , the best estimate of the alignment accuracy is applied. This is the result of studies from samples of straight tracks obtained in periods of collision data taken with no magnetic field in the muon system. The constraints on Δp_2^{MS} are reported on Table 1.

Table 1. Constraints on the intrinsic resolution term

η region	Constraint on Δp_2^{MS} (TeV ⁻¹)
barrel	0.143 ± 0.030
transition	0.312 ± 0.050
end-caps	0.200 ± 0.050
CSC/No-TRT	0.408 ± 0.050

4 Combined fit results

The constraints on the Δp_i parameters are applied in the combined fit by adding a penalty term $\sum_i \left(\frac{\Delta p_i - a_i}{\sigma_{a_i}} \right)^2$ to the total χ^2 being minimized, where a_i is the expectation value and σ_{a_i} the associated uncertainty for each of the constrained Δp_i parameters. The fitted correction parameters are provided in Table 2 together with their statistical and systematic uncertainties. Figure 1 shows an example of Z

Table 2. Set of corrections to be applied on the p_T parametrization of the simulated resolution in the MS and ID to reproduce the one in data. Systematic errors on the transition region are due to a different definition of the region itself ($1.2 < |\eta| < 1.7$)

η region	Δp_1^{MS} (%)	Δp_2^{MS} (TeV ⁻¹)
barrel	1.80 ± 0.05	0.095 ± 0.016
transition	3.17 ± 0.15 ± 0.22	0.250 ± 0.026 ± 0.067
end-caps	1.23 ± 0.11	0.169 ± 0.069
CSC/No-TRT	0.52 ± 0.58	0.453 ± 0.028

η region	Δp_1^{ID} (%)	Δp_2^{ID} (TeV ⁻¹)
barrel	0	0.283 ± 0.011
transition	0	0.736 ± 0.022 ± 0.567
end-caps	0	0.871 ± 0.017
CSC/No-TRT	0	0.050 ± 0.001

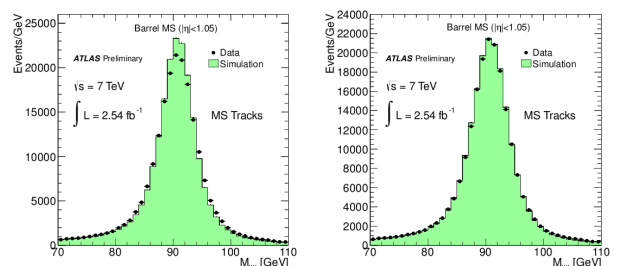


Fig. 1. Examples of Z lineshape fit for MS tracks in the barrel region, before (on the left) and after fit (on the right).

lineshape fit for MS tracks in the barrel region, before (left) and after (right) the fit.

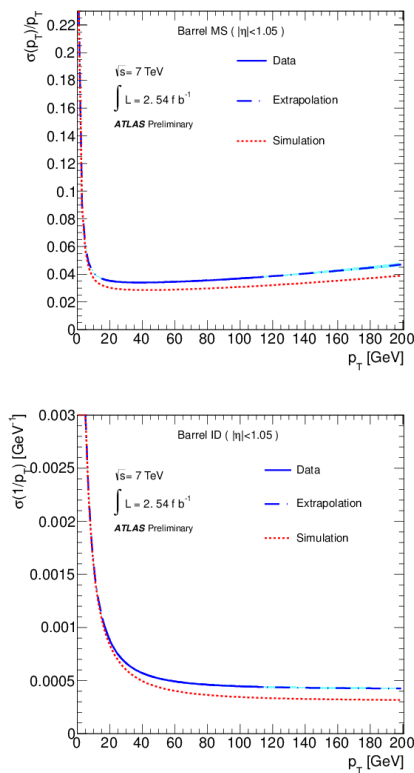
The values of the correction parameters quantify the increase in momentum resolution in data when compared to simulation. The full parametrization of the experimental momentum resolution is obtained by quadratically adding the uncorrected simulated resolution terms of equations 1-3 and the corresponding parameters from Table 2. The results for the full parametrization are listed in Table 3.

Table 3. Resolution parametrization as defined in equations 1-3 in the MS and ID.

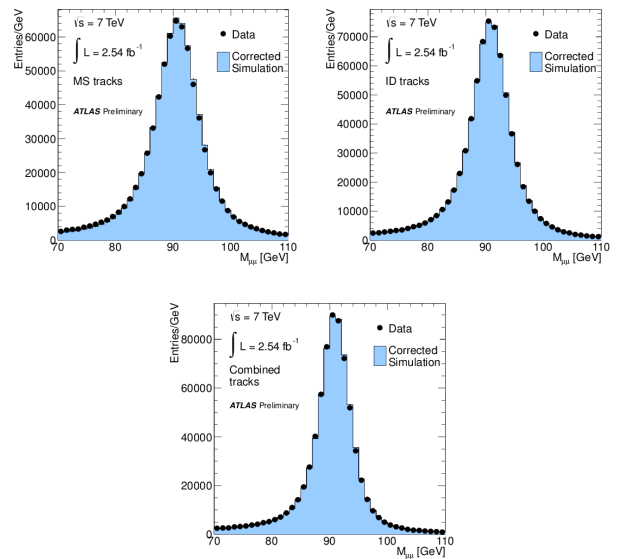
η region	p_0^{MS} (TeV)	p_1^{MS} (%)	p_2^{MS} (TeV ⁻¹)
barrel	0.25 ± 0.01	3.27 ± 0.05	0.168 ± 0.016
transition	0	6.49 ± 0.26	0.336 ± 0.072
end-caps	0	3.79 ± 0.11	0.196 ± 0.069
CSC/No-TRT	0.15 ± 0.01	2.82 ± 0.58	0.469 ± 0.028
η region	p_0^{ID} (TeV)	p_1^{ID} (%)	p_2^{ID} (TeV ⁻¹)
barrel	n.a	1.55 ± 0.01	0.417 ± 0.011
transition	n.a	2.55 ± 0.01	0.801 ± 0.567
end-caps	n.a	3.32 ± 0.02	0.985 ± 0.019
CSC/No-TRT	n.a	4.86 ± 0.22	0.069 ± 0.003

5 Measured resolutions as a function of p_T

The parametrized resolution as a function of p_T for the barrel region, obtained using the values of the parameters from the combined fits, are shown in figure 2 for the MS and the ID. The resolution curves for experimental data (in blue) are compared to those from uncorrected parameters obtained for the simulation (in red). To indicate the


Fig. 2. Resolution curve from the fitted parameter values on the MS (top) and the ID (bottom) in collision data and simulation as a function of the muon p_T , for the barrel region. The solid blue line shows determinations based on data, the dashed blue line shows the extrapolation to p_T range not accessible in this analysis and the dashed red line shows the determinations from simulation.

goodness of the simulation correction provided in section 4, figure 3 shows the distribution of the di-muon invariant mass in the Z region after applying the corrections, for MS, ID and combined tracks.


Fig. 3. Di-muon invariant mass comparison in the Z boson mass range between collision data (dots) and simulation (full histogram), after correcting the simulated muon p_T , in the full range of η . From top left to bottom: MS, ID and combined measurements are shown.

6 Conclusions

A determination of the muon momentum resolution is presented for the integrated luminosity of 2.54 fb^{-1} collision data collected in 2011 with the ATLAS detector. $Z \rightarrow \mu\mu$ decays have been used to evaluate the resolution as a function of the muon p_T and η , for both the MS and the ID. The momentum resolutions were measured on the experimental data and compared with the simulation. Results obtained present an improvement of the resolution and the alignment with respect to those obtained with 2010 data [7].

References

1. ATLAS Collaboration, *The ATLAS Experiment at the CERN Large Hadron Collider*, JINST **3** (2008) S08003
2. ATLAS Collaboration, *Determination of the muon reconstruction efficiency in ATLAS at the Z resonance in p-p collisions at $\sqrt{s} = 7 \text{ TeV}$* , ATLAS-CONF-2011-008 (2011).
3. ATLAS Collaboration, *Commissioning of the ATLAS Muon Spectrometer with Cosmic Rays*, Eur.Phys.J. **C 70**, (2010) 875.
4. ATLAS Collaboration, *The ATLAS Inner Detector commissioning and calibration*, Eur.Phys.J. **C 70**, (2010) 787.
5. ATLAS Collaboration, *Study of the Material Budget in the ATLAS Inner Detector with K_S^0 decays in collision data at $\sqrt{s}=900 \text{ GeV}$* , ATLAS-CONF-2010-019 (2010).
6. ATLAS Collaboration, *Studies of the performance of the ATLAS detector using cosmic-ray muons* Eur.Phys.J. **C71** (2011) 1593.
7. ATLAS Collaboration, *ATLAS Muon Momentum Resolution in the First Pass Reconstruction of the 2010 p-p Collision Data at $\sqrt{s} = 7 \text{ TeV}$* , ATLAS-CONF-2011-046 (2011).